

# 1 Improved Metabolite Prediction Using Microbiome Data-Based 2 Elastic Net Models 3 4

5 **Jialiu Xie<sup>1,2</sup>, Hunyong Cho<sup>1</sup>, Bridget M. Lin<sup>1</sup>, Malvika Pillai<sup>3</sup>, Lara H. Heimisdottir<sup>4</sup>,**  
6 **Dipankar Bandyopadhyay<sup>5</sup>, Fei Zou<sup>1</sup>, Jeffrey Roach<sup>6</sup>, Kimon Divaris<sup>4</sup>, Di Wu\*<sup>1,3</sup>.**

7 **Affiliations**

8 <sup>1</sup>Department of Biostatistics, Gillings School of Global Public Health, University of North  
9 Carolina at Chapel Hill, Chapel Hill, USA

10 <sup>2</sup>Department of Genetics, School of Medicine, University of North Carolina at Chapel Hill,  
11 Chapel Hill, USA

12 <sup>3</sup>Division of Oral & Craniofacial Health Sciences, School of Dentistry, University of North  
13 Carolina, Chapel Hill, NC, USA

14 <sup>4</sup>Division of Pediatric and Public Health, Adams School of Dentistry, University of North  
15 Carolina, Chapel Hill, NC, USA

16 <sup>5</sup>Department of Biostatistics, Virginia Commonwealth University, Richmond, VA, USA

17 <sup>6</sup>Research Computing, University of North Carolina, Chapel Hill, NC, USA

18 **\*Corresponding author:**

19 Di Wu

20 Department of Biostatistics, Gillings School of Global Public Health, University of North Carolina  
21 at Chapel Hill, Chapel Hill, USA

22 Division of Oral & Craniofacial Health Sciences, School of Dentistry, University of North  
23 Carolina, Chapel Hill, NC, USA

24 E-mail address: dwu@unc.edu.

25

26

27

28

29

30

31

32

33

34

35

36

37

38

39

40

41

42

43

44 **Abstract**

45

46 Microbiome data are becoming increasingly available in large health cohorts yet metabolomics  
47 data are still scant. While many studies generate microbiome data, they lack matched  
48 metabolomics data or have considerable missing proportions of metabolites. Since metabolomics  
49 is key to understanding microbial and general biological activities, the possibility of imputing  
50 individual metabolites or inferring metabolomics pathways from microbial taxonomy or  
51 metagenomics is intriguing. Importantly, current metabolomics profiling methods such as the  
52 HMP Unified Metabolic Analysis Network (HUMAnN) have unknown accuracy and are limited  
53 in their ability to predict individual metabolites. To address this gap, we developed a novel  
54 metabolite prediction method, and we present its application and evaluation in an oral  
55 microbiome study. We developed ENVIM based on the Elastic Net Model (ENM) to predict  
56 metabolites using microbiome data. ENVIM introduces an extra step to ENM to consider  
57 variable importance scores and thus achieve better prediction power. We investigate the  
58 metabolite prediction performance of ENVIM using metagenomic and metatranscriptomic data  
59 in a supragingival biofilm multi-omics dataset of 297 children ages 3-5 who were participants of  
60 a community-based study of early childhood oral health (ZOE 2.0) in North Carolina, United  
61 States. We further validate ENVIM in two additional publicly available multi-omics datasets  
62 generated from studies of gut health and vagina health. We select gene-family sets based on  
63 variable importance scores and modify the existing ENM strategy used in the MelonPan  
64 prediction software to accommodate the unique features of microbiome and metabolome data.  
65 We evaluate metagenomic and metatranscriptomic predictors and compare the prediction  
66 performance of ENVIM to the standard ENM employed in MelonPan. The newly-developed  
67 ENVIM method showed superior metabolite predictive accuracy than MelonPan using  
68 metatranscriptomics data only, metagenomics data only, or both of these two. Both methods  
69 perform better prediction using gut or vagina microbiome data than using oral microbiome data  
70 for the samples' corresponding metabolites. The top predictable compounds have been reported  
71 in all these three datasets from three different body sites. Enrichment of prediction some  
72 contributing species has been detected.

73

74 **Keywords:** microbiome, metatranscriptome, metabolome, prediction, elastic net, random forest

75

76

77 **INTRODUCTION**

78

79 The importance of the human microbiome in health and disease is undeniable; site-specific  
80 microbial communities interact both with the environment and the host and influence numerous  
81 biological processes (1). Aside from the logical interest in understanding the microbiome's  
82 composition, measuring and understanding its associated metabolic activities is arguably of  
83 utmost biological relevance. Recent studies have linked the metabolome with several important  
84 health conditions including inflammatory bowel disease (IBD)(2), obesity and type II diabetes  
85 (3), cholesterol levels (4), and early childhood dental caries (ECC)(5). Despite the rapidly  
86 increasing availability of microbiome data in large health cohorts, metabolomics data are still  
87 scant. This is an important limitation because the lack of, or considerable missingness of,  
88 metabolite information in microbiome studies can diminish their potential in inferring functions  
89 and important biological targets.

90 It follows that methods that help fill in the functional information gaps in microbiome studies are  
91 valuable and necessary. Because “matched” microbiome and metabolome datasets are extremely  
92 scant, most current methods rely on metabolic pathway inferences from taxonomic and  
93 metagenomic data, such as in the HMP Unified Metabolic Analysis Network (HUMAnN) (6).  
94 While the value of this approach is well-documented for the analysis of some microbial consortia  
95 (e.g., the human gut) (2, 7), HUMAnN cannot make predictions for individual metabolites.  
96 Moreover, its accuracy has not been benchmarked and its performance in other microbial  
97 communities with distinct ecology and function (e.g., the oral cavity) remains unknown. This is  
98 important because measured metabolomes at different body sites may include, besides the  
99 products of microbial metabolism, biochemical contributions from the host and the environment  
100 (e.g., dietary sugars in the study of dental biofilm(5)). Although an accurate determination of  
101 metabolite sources may not always be possible, predictions of these biofilm metabolites using  
102 microbiome information are highly desirable.

103 Along these lines, in 2016, Noecker and colleagues (8) added to the available analytical toolbox  
104 by leveraging 16S rRNA data. Their method enabled model-based integration of metabolite  
105 observations and species abundances using taxonomy and paired metabolomics data from ~70  
106 vaginal samples. More recently, MelonnPan (9) was developed to obtain metabolomic profiling  
107 of microbial communities using amplicon or metagenomic sequences. This new method was  
108 motivated and applied in the context of paired microbiome and metabolome data in the context  
109 of an IBD cohort.

110 The motivation for the present new method development is to improve existing analytical  
111 approaches available for metabolite prediction and functions using microbiome data (10). To this  
112 end, we leverage existing microbiome and metabolome data from a study of early childhood oral  
113 health investigating ECC, a study of the human gut investigating IBD, and a study of vaginal  
114 health. The elastic net model (ENM, also used in MelonnPan), compared to LASSO or ridge  
115 regression, benefits from keeping both the singularities at the vertices, which is necessary to  
116 accommodate data sparsity, and the strict convex edges for grouping among correlated variables.  
117 Inspired by MelonnPan and MIMOSA, we propose an improved prediction method for  
118 individual metabolites using microbiome information in the same biological samples (as matched  
119 samples or paired samples), called "Elastic Net Variable Importance Model (ENVIM)". It  
120 improves upon ENM algorithms by weighing microbial gene features using random forest  
121 variable importance (VI) to enhance the contribution of most prediction-informative genes.  
122 ENVIM outputs predicted metabolites from matched microbiome samples, as well as genes and  
123 their weights informing metabolite prediction.

124 In this paper, we present the development, application, and evaluation of the new method  
125 ENVIM. We compare it against MelonnPan in three datasets generated from oral, gut, and  
126 vaginal samples, so that we can also compare the metabolite prediction among different body  
127 sites. The predictors can be three different gene family data types, e.g., metagenome only,  
128 metatranscriptome only, and the combination of both metagenome and metatranscriptome data.  
129 The top predictable compounds have been reported in all these three datasets from three  
130 different body sites. Enrichment of some prediction contributing species has been detected.  
131  
132

## 133 MATERIAL AND METHODS

### 134 1. Cohort and data description

136 In the following section, we describe the microbiome and metabolome data used for the new  
137 method development and application, alongside the three contributing studies.

138

### 139 ***ZOE 2.0 study data***

140 ZOE 2.0 is a community-based molecular epidemiologic study of early childhood oral health in  
141 North Carolina (11, 12). The study collected clinical information on preschool-age children's  
142 (ages 3-5) dental cavities (i.e., referred to early childhood caries or ECC) (13) and supragingival  
143 biofilm samples from a sample of over 6,000 children (14). A subset of participants' biofilm  
144 samples underwent metagenomics, metatranscriptomics, and metabolomics analyses, under the  
145 umbrella Trans-Omics for Precision Dentistry and Early Childhood Caries or TOPDECC  
146 (accession: phs002232.v1.p1) (11). As such, metagenomics (i.e., shotgun whole genome  
147 sequencing or WGS), metatranscriptomics (i.e., RNA-seq), and global metabolomics data (i.e.,  
148 ultra-performance liquid chromatography-tandem mass spectrometry) (5, 15, 16) from  
149 supragingival biofilm samples of ~300 children, paired with clinical information on ECC are  
150 available. After exclusions due to phenotype and metabolite missingness described in a previous  
151 publication (5), the joint microbiome-metabolome data include 289 participants. There are 503  
152 known metabolites included in the ZOE 2.0 dataset. Metagenomics and metatranscriptomics data  
153 in reads per kilobase (RPK) were generated using HUMAnN 2.0. Here, we use species-level  
154 (205 species), gene-family (403K gene families), pathway (397 pathways), and metabolome (503  
155 metabolites) data.

156

### 157 ***Lloyd-Price study data***

158 The Lloyd-Price dataset (2) was obtained from the Inflammatory Bowel Disease multi-omics  
159 database (<https://ibdmd.org>). It is derived from a longitudinal study that sought to generate  
160 profiles of different types of omics data among 132 participants for one year and up to 24 time  
161 points. The study's several different types of omics data include WGS shotgun metagenomics,  
162 RNA-seq metatranscriptomics, and metabolomics. The corresponding metadata include  
163 demographic information such as occupation, education level, and age. These gut microbiome  
164 data are in counts per million (CPM) and were derived using functional profiles 3.0 in  
165 HUMAnN3.0. For this study, we merged data of individual gene families for 1638 samples for  
166 130 subjects, and individual metatranscriptomics gene families for 817 samples for 109 subjects,  
167 respectively. The merged metagenomics gene families data include about 2,741K gene families  
168 and 1580 samples. Merged metatranscriptomics gene families data include about 1,079K gene  
169 families and 795 samples. The metabolomics data were generated using LC-MS and include  
170 81,867 metabolites and 546 samples for 106 subjects. Most metabolites have not been annotated  
171 into known biochemicals and thus were excluded from prediction. After limiting the dataset to  
172 known metabolites and removing "redundant ions" in "HMDB" ID, there remained 526  
173 metabolites to be predicted.

174

### 175 ***Mallick study data***

176 The Mallick data (9) comprised the main real-life dataset used in the development of the  
177 MelonPan method (9). They are derived from gut microbiome WGS shotgun sequencing from  
178 two cross-sectional IBD cohort studies, namely the Prospective Registry cohort for IBD Studies  
179 at the Massachusetts General Hospital (PRISM) and the Netherlands IBD cohort (NLIBD).  
180 Gene-family data in RPK units were derived using HUMAnN2.0 and normalized to reads per  
181 kilobase per million sample reads (RPKM). The raw metagenomics gene-family dataset includes

182 1 million gene families. The investigators (9) filtered out genes with low abundance and  
183 prevalence resulting in a processed dataset of 811 genes available in the R package *Melonpan*  
184 (*melonpan.training.data* and *melonpan.test.data*) for 222 total subjects. The microbiome data  
185 have been pre-processed and normalized into relative abundance. The metabolite abundance data  
186 (8,848 metabolites and 220 subjects) have been made available by Franzosa et al (17). Those  
187 authors used 466 metabolites for analyses, a subset that was confirmed experimentally against  
188 laboratory standards prior to application in *Melonpan*. In the present study, we use information  
189 from these 466 metabolites to compare the power of the new ENVIM method against  
190 *Melonpan*. To accomplish this, we normalized the metabolite abundance data for all 8848  
191 metabolites into relative abundance (compositional format). Among them, we used the same 466  
192 metabolites with laboratory standards as selected in the paper of *Melonpan* (9). Data  
193 missingness is not an issue in the Mallick metabolome data.  
194

## 195 **2. Metabolomics data pre-processing and normalization**

196 An overview of the approach for metabolome data is presented in **Figure 1** and elaborated in  
197 detail below.

198  
199 **Metabolomics missing data imputation: ZOE 2.0 and Lloyd-Price studies.** The proportions of  
200 missing metabolite data are small in the ZOE 2.0 and Lloyd-Price studies. In ZOE 2.0, 87% of  
201 metabolites have some missing data whereas 58% have missing values in Lloyd-Price. To  
202 address missingness in these two cohorts, we applied a rigorous feature-wise Quantile  
203 Regression Imputation of Left-Censored data (QRILC)(18) to impute missing metabolite values  
204 and avoid underestimated metabolite-level variance, as in a previous publication (5). All 503  
205 metabolites in ZOE 2.0 have <90% missing data among the 289 included participants. We  
206 applied a similar preprocessing filter for the Lloyd-Price data (i.e., removing outlier subjects,  
207 **SuppFigure 1**), resulting in the exclusion of 15 outlier subjects with the largest numbers of  
208 missing metabolite values, as well as outlier metabolites with >90% missing values.  
209 Consequently, we carried forward to analyze 522 metabolites in 531 samples from the Lloyd-  
210 Price data.

211 The application of the QRILC imputation method departed from a natural log data  
212 transformation for the imputation step and an exponentiation to back transform the data to RPK  
213 (in ZOE 2.0) or CPM (in Lloyd-Price) scales. Because MelonPan requires metabolite data to be  
214 inputted as compositional, we converted RPK and CPM imputed data to a compositional format  
215 before predictive modeling.

## 216 **Metabolites Filtered by Metabolic Pathways (ZOE 2.0, Lloyd-Price and Mallick)**

217 We used the MetaCyc database to retain only “reactive” metabolites. To achieve this, we  
218 considered metabolites’ membership in any MetaCyc metabolic pathway, reflecting reactions  
219 between bacteria and metabolites, and carried out the following steps:  
220

221 (1). In the MetaCyc database, we identify metabolites in each of the pathways predicted by  
222 metagenomics data in Functional Profile 2.0 generated by HUMAnN 2.0 (ZOE 2.0 and Mallick  
223 data) and Functional Profile 3.0 generated by HUMAnN 3.0 (Lloyd-Price data).  
224  
225

227 (2). We used metabolites labels (KEGG id, HMDB, PUBCHEM, and metabolite name, provided  
228 in Metabolome data annotation, provided by manufacturer) in each of the three datasets, as the  
229 mapping IDs for each metabolite.

230

231 (3). In MetaCyc, regardless of the metabolite label, only one unique MetaCyc “weblink” or  
232 universal mapping id is returned if the metabolite is in the database. This way, reactive  
233 metabolites identified in step 1 can be matched with metabolites identified in step 2.  
234 This way, we identify metabolites that are in the observed pathways. Finally, we filter out  
235 metabolites with low abundance (metabolites with mean relative abundance  $<10^{-4}$ ) and low  
236 prevalence (metabolites with  $>10\%$  non-zero values). Consequently, there were 149 metabolites  
237 in pathways in ZOE 2.0, 125 in Lloyd-Price, and 251 in the Mallick data. Of note, no pathway  
238 information exists in the Mallick data. To compare the prediction of metabolites in pathways  
239 with the prediction of all metabolites, we considered both sets of metabolites in our analyses.  
240

241

### 242 3. Microbiome data pre-processing and normalization

243 An overview of the approach for microbiome data is presented in **Figure 1** and elaborated in  
244 detail below. First, we matched gene family-level microbiome data with metabolome data by  
245 participant or sample unique identifier. Then, the scaled (RPK, RPKM, or CPM) gene family  
246 abundances were converted to compositional data, relative to the total per sample. Then, we  
247 filtered out gene family features with low relative abundance (mean relative abundance  $<5 \times 10^{-5}$ )  
248 and low prevalence (percentage of zeros in  $>90\%$  of the samples) and thus kept 0.5% - 5% of  
249 gene family features. The same procedures were performed for both metatranscriptomics (briefly  
250 referred to as “RNA” thereafter) and metagenomics data (briefly referred to as “DNA” hereafter)  
251 thereafter, respectively. When both DNA and RNA data (briefly as “BOTH” hereafter) are  
252 considered predictors, a gene name may correspond to two “gene features”, one for each data  
253 type. The same data pre-processing and normalization procedures were followed for three  
254 cohorts, with sample sizes and feature numbers presented in **Table 1**. To prevent overfitting  
255 when evaluating ENM and ENVIM, we divided samples into training (75% of subjects) and  
256 testing datasets (25% of subjects).

257

### 258 4. The existing ENM method for microbiome data-based metabolite prediction

259

260 As mentioned previously, the existing method available for predicting metabolite abundance  
261 using metagenomics data is MelonPan(9) (Model-based Genomically Informed High-  
262 dimensional Predictor of Microbial Community Metabolic Profiles). In this study, in MelonPan  
263 we used all filtered metagenomic gene family features in the 10-fold cross-validated elastic net  
264 model (ENM)(19) to predict metabolite abundance (**Equation 1**).

265

266 However, using all filtered metagenomic gene family features in the model may dilute the effect  
267 of some important gene family features contributing to the prediction of metabolite abundance.  
268 This limitation can be improved upon, and therefore, in this paper, we set out to improve the  
269 ENM and develop a new algorithm.

270

271 The MelonPan software was downloaded from Github  
(<https://github.com/biobakery/melonpan>) or in *Melonpan* Package in R, the CSV output file

272 “Predicted\_Metabolites.txt” (Train) and “MelonnPan\_Predicted\_Metabolites.txt” (Test) are used  
273 as the prediction results of MelonnPan.

274

275

276 Elastic net model (ENM) assumes the model,

$$y_i = x_i' \beta + \epsilon_i,$$

277 where  $\beta = (\beta_0, \beta_1, \dots, \beta_p)'$  and  $\hat{\beta}$ , the ENM estimator of  $\beta$ , is found by minimizing the objective  
278 function of ENM,

$$L_{ENM} = \frac{1}{2N} \sum_{i=1}^N (y_i - x_i' \beta)^2 + \lambda \sum_{j=1}^p \left\{ \frac{1-\alpha}{2} \beta_j^2 + \alpha |\beta_j| \right\}.$$

279

## 280 Equation 1

281

282

## 283 5. Evaluation Methods

284

285 We used Cohen’s criterion (20), to define Well-Predicted (WP) metabolites as those with  
286 Spearman correlation  $\geq 0.3$ , and those with correlation  $< 0.3$  as poorly predicted. The predictive  
287 performance of the new method ENVIM is evaluated by comparing it against MelonnPan.  
288 Additionally, we compare Spearman correlations and mean square error (MSE) between the  
289 predicted and observed metabolites in both the training stage and the testing stage for all the  
290 three datasets and both methods.

291

## 292 RESULTS

293

### 294 1. The improved ENM based on variable importance score (ENVIM)

295

296 The new algorithm is based on ENM, as the Elastic Net Variable Importance Model (ENVIM)  
297 (**Equation 2**). The strategy in ENVIM and the comparison between ENM and ENVIM are  
298 shown in **Figure 2**. Because ENM assumes that both independent and dependent variables  
299 follow a normal distribution, we rank-transform each gene family’s feature to a normal  
300 distribution by using the *rntransform* (21) function in the R package *GENABEL* for training data  
301 and testing data, respectively. The training metabolite abundance data are transformed to a  
302 normal distribution by Box-Cox transformation. After fitting the model in the training data,  
303 predicted metabolite abundances are transformed back to relative abundance with  $\lambda$  being  
304 determined by the training metabolite abundance data.

305

306 Including all gene families into the model could make the cross-validated MSE larger, whereas  
307 including only a small part could make the error larger. Therefore, to identify a model with the  
308 minimum cross-validated error one needs to iterate different numbers of gene families. Because  
309 we prioritize gene families with high importance relative to metabolites, we use a nonlinear  
310 regression model to determine the importance of gene families for each metabolite. We train a  
311 cross-validated random forest model(22) by using the training data and use *varImp* function in  
312 the *caret* package(23) in R to find the scaled importance score (0-100) between each independent  
313 feature and the metabolite abundance. We introduce a unique step that uses the scaled variable

314 importance score to classify gene families in different category intervals into the ENM, for  
315 example, gene families from 90 to 100. We use *glmnet* (24) package in R to run cross-validated  
316 ENM and choose penalty parameters for each model.

317

318 *In the training stage*, we divide the importance score from 0-100 into 10 category intervals (90-  
319 100, 80-100,..., 10-100, 0-100) and remove the intervals without gene families. We consider  
320 different sets of gene families with different importance scores into the ENM. Gene families are  
321 the independent variables, and metabolite abundances are the dependent variables. For each set  
322 of gene families, we conduct a 10-fold cross-validated ENM and build 10 models with different  
323 values of the tuning parameter  $\lambda$ , ranging from 0 to 1. For each model, we measure the MSE  
324 between the measured metabolite abundance and the predicted values to determine the best  
325 model (i.e., the model with the lowest MSE). To maintain reproducibility, we maintain the same  
326 random seed and permute the same fold index number in the ENM.

327

328 *In the testing stage*, for the prediction of each metabolite, we use a weight matrix of coefficients  
329 of gene families from the best model with the lowest MSE identified during the training stage.  
330 Because we previously transformed the compositional metabolite abundance data into  
331 compositional metabolite abundance per hundred and used Box-Cox transformation, we  
332 transform the predicted metabolite abundance data back to the original scale based on  $\lambda$   
333 calculated in the training step. We evaluate the prediction of testing metabolite abundance by  
334 using the Spearman correlation between measured and predicted metabolite abundance data.

335

336 ENVIM assumes the following model:

$$y_i = x_i' \beta + \epsilon_i,$$

337 where  $\beta = (\beta_0, \beta_1, \dots, \beta_p)'$  and  $\hat{\beta}^{ENVIM} = \operatorname{argmin}_{\beta} \min_{k \in \mathcal{E}} L_{ENVIM}(k)$ , the ENVIM estimator  
338 of

339  $\beta$ , is found by minimizing over  $k$  and  $\beta$  the objective function,

$$L_{ENVIM}(k) = \frac{1}{2N} \sum_{i=1}^N (y_i - x_i' M_k \beta)^2 + \lambda \sum_{j=1}^p s_{k,j} \left\{ \frac{1-\alpha}{2} \beta_j^2 + \alpha |\beta_j| \right\}.$$

340 where we define  $VI_j$  as the variable importance score for the  $j$ th variable given by a random  
341 forest,  $S_k = \{s_{k,j}\}_j^p = I\{VI_j \geq k\}_j^p$  is the variable selection indicator vector giving 1 if the  
342 importance score for the  $j$ th variable is larger than the importance score  $k$ ,  $M_k = \operatorname{diag}\{(1, S_k')\}$  is  
343 the corresponding diagonal variable selection matrix that includes the intercept term, and  $\mathcal{E}$  is a  
344 set of the candidate  $k$  values.  $\mathcal{E}$  is defined adaptively so that it covers the range of the variable  
345 importance scores reasonably. In our analysis, we set  $\mathcal{E} = \{0, 10, 20, \dots, 90\}$ .

346

## 347 Equation 2

348

349 **In the following sections, we present three key differences between MelonnPan and  
350 ENVIM for predicting individual metabolites (Figure2).**

351

352 *(1) Transformation of metabolite abundance data into a normal distribution.*

353 To meet the assumption of ENM, MelonnPan transforms relative metabolite abundances with the  
354 arcsin square root operator, whereas we use Box-Cox transformation in ENVIM. To test

355 normality, we compare the p-values of the Shapiro test statistics for both Box-Cox (**Equation 3**)  
356 and the arcsin square root transformations of metabolite abundances. In **Figure 3a**, the boxplots  
357 illustrate the distribution of -log10 of the p-values for all three data sets transformed by Box-Cox  
358 and arcsin square root and demonstrate that -log10 p-values for the Box-Cox transformation are  
359 greater than those applied with the arcsin square root transformation. In **Figure 3b**, in the scatter  
360 plot, -log10 p-values of almost all the metabolites applied with the Box-Cox transformation are  
361 more normally distributed than those applied with the arcsin square root transformation,  
362 implying that Box-Cox transformation yields better normal approximation than the arcsin square  
363 root transformation for most of the metabolites.

364

365

366 Box-Cox transformation

$$y = \begin{cases} \frac{y^\lambda - 1}{\lambda}, & x \neq 0, \\ \log(y), & x = 0 \end{cases}$$

367 where  $y$  is the relative abundance.

368

### 369 **Equation 3**

370

371 *(2) Different sets of gene families are carried forward to the prediction model.*

372 MelonnPan uses all gene families in the training data in the ENM and ultimately predicts  
373 metabolites in the testing stage using the same features. However, regressing against all gene  
374 families may dilute the effect of important gene families. Thus, unlike MelonnPan, we use a  
375 variable importance criterion to select different sets of gene families and include them in the  
376 prediction models.

377

378 *(3)  $\alpha$  range in ENM*

379 *Alpha* ( $\alpha$ ) is the weight between  $L_1$  and  $L_2$  penalty terms in the ENM, and in combination with  $\lambda$   
380 values, the set of values that minimizes the 10-fold cross-validated MSE (Equation 1) is chosen.  
381 When  $\alpha$  is 0, the model reduces to a ridge regression model which has the advantage of dealing  
382 with highly correlated independent variables; when  $\alpha$  is 1, the model becomes a lasso regression  
383 model which has a variable selection capacity; when the  $\alpha$  is between 0 to 1, the model includes  
384 the advantages of ridge regression and lasso regression. In MelonnPan, the range of  $\alpha$  values  
385 does not include 0 and 1, which excludes either the Ridge or LASSO regression models, and it  
386 may not consider variables with high importance. The penalty term *alpha* in our ENVIM  
387 includes 0 and 1. By allowing a larger range of  $\alpha$  we can include the case that is the Ridge  
388 regression model that does not exclude variables with high importance.

389

390 The ENVIM software written in R statistical language is available in Github  
391 (<https://github.com/jialiux22/ENVIM>). The "ENVIM\_predict" function is for metabolite  
392 prediction only, and the ENVIM function is for metabolite prediction and evaluation given  
393 metabolomics data in the testing set is also available. Both will output weight matrix. The weight  
394 matrix in testing has the same values as in training if they have the same number of genes.  
395 Usually, testing has a smaller number of genes to be used for prediction, so the weight matrix in  
396 testing can be a subset of the weight matrix in the training set due to the smaller number of genes  
397 in the testing set.

398

## 399 2. Method Comparison for Prediction of Individual Metabolites in Three Datasets

400

401 **Correlation-based method comparison.** We used microbial gene family data to predict the  
402 individual metabolites in the matched samples (that are from the same biological sample in that  
403 one proportion is for microbiome and the other is for metabolome). We compared the prediction  
404 results between ENVIM and MelonnPan, in terms of Spearman correlation and mean square  
405 error (MSE) between predicted and observed values of each of the filtered metabolites, in three  
406 datasets (ZOE 2.0, Mallick data, and Lloyd-Price data) at each of the three data types of  
407 microbial gene families as the DNAseq, RNAseq, and BOTH (of RNA and DNA). MSE in the  
408 testing set is for comparison between methods (**Supplemental Figure 2**).

409

410 We have summarized the prediction results (**Table 2**, **Figure 4**) for all metabolites in terms of  
411 Spearman's correlation according to three aspects: method comparison, modality comparison,  
412 and microbial community (i.e., body site) comparison. Overall, ENVIM produces higher  
413 percentages of well-predicted metabolites than MelonnPan in all three data cohorts, in both  
414 testing and training sets, and for DNA, RNA, and BOTH when available (**Table 2**).

415

416 In general, RNA gene family data produce higher percentages of well-predicted metabolites than  
417 DNA data. In Lloyd-Price data, RNA-only data typically give higher percentages of well-  
418 predicted metabolites. In ZOE 2.0 and Lloyd-Price data, both DNA and RNA predictors produce  
419 similar percentages but are not always superior to the DNA-only or RNA-only data-based  
420 predictors. However, results emanating from both DNA and RNA predictors are never the worst.  
421 Not surprisingly, the well-predicted percentage of metabolites in testing sets is lower than in the  
422 training set (**Table 2**). The boxplots of Spearman correlations between the predicted and  
423 observed metabolites for all metabolites (**Figure 4**) show the overall distribution of Spearman  
424 correlation and suggest that the correlation between the ENVIM-predicted and the observed  
425 metabolites is higher in RNA than in DNA, but slightly lower than in both DNA and RNA. In  
426 testing, MelonnPan only predicts the predictable metabolites (defined as Well-Predicted  
427 metabolites in Training set, last columns in **Table 2**); while it is not appropriate to compare the  
428 correlation distribution for all metabolites as in **Figure 4** for MelonnPan. When comparing the  
429 distribution of correlation (**Figure 4**) between the ENVIM-predicted and the observed  
430 metabolites in ZOE2.0 and Lloyd-Price, the combination of both DNA and RNA appears to have  
431 higher correlations than the DNA only or RNA only in the training set. In testing, RNA data  
432 produce the highest median correlation. All three gene family data result in similar correlations  
433 in ZOE 2.0. It must also be noted that the highest proportion of well-predicted metabolites is  
434 found in the gut microbiome (Lloyd-Price) study, then in the vagina microbiome (Mallick study),  
435 and the lowest was in the supragingival dental biofilm (ZOE 2.0 study) (**Table 2**). Because in  
436 both the Lloyd-Price and Mallick datasets prediction correlations are higher than in ZOE 2.0  
437 (**Figure 4**), it is reasonable to suggest better metabolite prediction in these sites and microbial  
438 communities than in the oral cavity.

439

440 Besides comparing MelonnPan and ENVIM in terms of percentages of well-predicted  
441 metabolites, one can directly compare the correlations of each predictable metabolite that is  
442 predicted by both methods (**Figures 5 and 6**). In the training set (**Figure 5**), all DNA, RNA,  
443 BOTH DNA, and RNA, and in all three datasets, we find that the majority of these metabolites

444 have higher correlations in ENVIM compared to MelonnPan. The same holds in the testing set  
445 (**Figure 6**): most points are along the diagonal line but slightly above it, suggesting that  
446 metabolites predicted by ENVIM have higher correlations with the observed ones compared to  
447 those predicted by MelonnPan. We also find that there are more metabolites in the  
448 "ENVIM>0.3" category (blue) than in the "MelonnPan>0.3" category (red). This is a reflection  
449 of more well-predicted metabolites found after ENVIM than after MelonnPan prediction.  
450

### 451 **3. Methods comparison for prediction of individual metabolites in three datasets and the** 452 **context of observed metabolic pathways**

453  
454 Metabolites may be associated with the microbiome in the context of metabolic pathways that  
455 involve interactions between host, microbiome, and environment. We further test the methods'  
456 predictive power for metabolites that are found in microbiome data-based metabolic pathways  
457 generated by metagenomics and metatranscriptomics analysis in HUMANN2. Gene families are  
458 filtered by metabolic pathways as previously described in the methods section. All conclusions  
459 regarding the prediction of metabolites still hold in this scenario. Additionally, when comparing  
460 the percentages of well-predicted metabolites among all metabolites (first four columns of **Table**  
461 **2**) and the metabolites found in pathways (**Table 3**), we find higher predicted percentages for the  
462 latter.  
463

### 464 **4. Methods comparison based on MSE**

465  
466 We use boxplots to compare the mean square errors (MSE) between measured and predicted  
467 metabolite abundance between ENVIM and MelonnPan both for training and testing models,  
468 with application to training data and testing data for all three studies. We only compare well-  
469 predicted metabolites identified by MelonnPan in training because MelonnPan only generates  
470 results for these metabolites. The boxplot demonstrates that the distribution of MSE in the  
471 MelonnPan model is approximately the same as the distribution of MSE in ENVIM  
472 (**Supplemental Figures 2**). There is no significant MSE difference between ENVIM and  
473 MelonnPan suggesting that both models predict these metabolites well, but the advantage of  
474 ENVIM is that we can predict substantially more well-predicted metabolites than MelonnPan—a  
475 consequence of MelonnPan's inability to build a well-performing model in the training step.  
476  
477

### 478 **5. Prediction Results of Individual Metabolites and Gene Weights in ENVIM**

479  
480 The top 50 predicted metabolite compounds from ENVIM across three datasets are shown in  
481 **Figure 7**. For Lloyd-Price and ZOE 2.0, we choose the gene family data that has the best  
482 ENVIM prediction power to show their top predicted metabolites, which are the DNA gene  
483 family data (124 metabolites as 25% among NM, **Table 2**) in ZOE 2.0, and the RNA gene family  
484 data (393 metabolites as 75% among NM, **Table 2**) in Lloyd-Price. The Mallick study only has  
485 DNA data available for metabolite prediction. Lloyd-Price data and Mallick data have measured  
486 metabolites in >1 metabolome LC-MS platforms (see Data Description Section) so that one  
487 metabolite may appear >1 time in the top list, for example, the metabolite so-called Urobilin  
488 appeared in the top 50 for >1 time.

489 The summarized prediction results can be seen in **Supplemental Table 1**. To interpret the  
490 results, we take the carbohydrate pathway as an example that may provide the bacteria nutrition,  
491 so a few compounds have been well-predicted by the RNA gene data. We are aware the  
492 prediction in this paper is not about longitudinal causal relation but for mathematical prediction.  
493 Here we show four examples (**Figure 8A, B, C, D** for Trehalose, Maltose, Ribose Stachyose)  
494 that also have high Spearman correlation in the log10 scale of compositional data.  
495

496 **Gene list (Weight matrix) comparison across three datasets, in ENVIM (Supplemental Table**  
497 **2)**. We extract gene names that are non-zero in the weight matrix for each metabolite, dataset,  
498 and data type. We aim to compare gene names among three datasets and find the probability of  
499 predicting metabolites by using a different dataset. We find that there are not many overlapped  
500 genes ( $n < 10$ ) between ZOE 2.0 data and Lloyd-Price data (Data not shown).  
501

502 **Gene set enrichment analysis (GSEA) within Species in ZOE 2.0.** We perform gene set  
503 enrichment analysis to find the over-represented species of the gene families when we build the  
504 prediction model on metabolite abundance. We extract the weight matrix, merge the important  
505 gene families with non-zero values among all well-predicted metabolites. We get the summation  
506 of the rank of each gene family in the weight matrix based on the absolute value of the  
507 coefficient for each gene family. We use gene families data at the species level to find the  
508 species corresponding to those important gene families. For each species of bacteria, we compare  
509 the general difference in the cumulative distributions of gene families' rank scores between each  
510 species and background species and find Kolmogorov–Smirnov (KS) p-values. We use the  
511 Benjamini–Hochberg false discovery rate (FDR) approach to correct the p-values and get q-  
512 values. There are 36 species in ZOE 2.0 DNA data and 73 species of bacteria in ZOE 2.0 RNA  
513 data that show significantly ( $q < 0.05$ ) over-represented species during the gene set enrichment  
514 analysis (**Figure 9**).  
515

516 Here, we used a different procedure for the gene set enrichment tests compared to what  
517 MelonnPan (9) used. They pooled genes in genera instead of species, due to the small number of  
518 genes in each species in their prediction procedure. We keep many more genes than MelonnPan  
519 so that we can address the ranks of genes instead of the binary prediction power of genes (i.e.,  
520 whether a gene is used for prediction or not). Our GSEA strategy also can help avoid the bias to  
521 pick up the species that have larger numbers of genes.  
522  
523

## 524 **6. Computational speed (compare to others):**

525 Our developed method of improving ENM could run on the software on R and accurately predict  
526 metabolites. The mean prediction time for each metabolite for DNA gene families data is 5.2  
527 minutes for ZOE2 data (6.1 minutes for Lloyd-Price Data, 2 minutes for Mallick data); mean  
528 prediction time for RNA gene families data is 4.2 minutes for ZOE2 data (3.7 minutes for Lloyd-  
529 Price Data); mean prediction time for both DNA and RNA gene families data is 4.5 minutes for  
530 ZOE2 data (3.6 minutes for Lloyd-Price Data) with MacOS Big Sur Version 11.4.  
531  
532

## 533 **DISCUSSION**

535  
536 We propose a new computational method for metabolite prediction using microbiome data-based  
537 improved Elastic Net Models. We chose different gene-family sets based on SVM-based variable  
538 importance scores and modified the existing ENM to accommodate the unique features of  
539 microbiome and metabolome data. The newly developed method ENVIM predicts metabolites  
540 using metagenomics, metatranscriptomics, or both data types. We apply the algorithm in three  
541 datasets, i.e., ZOE 2.0, Mallick, and Lloyd-Price studies. These three studies are mostly all we  
542 can find that have both microbiome and metabolome data in the same matched samples, with  
543 reasonably large sample sizes. Our work is the first time that researchers can use microbiome  
544 data to predict metabolites in more than one study, and different body sites. In addition, ZOE 2.0  
545 and Lloyd-Price studies have both metagenomics and metatranscriptomics, so that we can for the  
546 first time, compare the prediction performance using the different gene family modalities (or  
547 called data types).  
548  
549 We evaluated metagenomic and metatranscriptomic predictors and compared the prediction  
550 performance between the previously developed MelonnPan and ENVIM, among DNA, RNA,  
551 and Both DNA and RNA gene families data using (1) the proportion of “well-predicted”  
552 metabolites defined as those with Spearman correlation between measured and predicted  
553 metabolite values  $> 0.3$ , (2) distribution of Spearman correlation and (3) MSE. The correlation  
554 suggests Both (using DNA and RNA jointly) provides robust prediction results that are never the  
555 worst among the three data types. Whether DNA or RNA have better prediction performance  
556 depends on the studies. The percentage of well-predicted metabolites is higher for metabolites  
557 that are in a metabolic pathway that is observed in microbiome data, and this supports the  
558 interaction between microbiome and metabolites may highly be related in known metabolic  
559 pathways. Across all datasets and data types, with or without the pathway filter, we find ENVIM  
560 always outperforms MelonnPan. We also find the prediction performance is better in Lloyd-Price  
561 and Mallick than in ZOE 2.0, which may suggest the association between microbiome and  
562 metabolites are stronger in the gut than in the oral cavity since oral metabolites may be more  
563 affected by environmental factors like food intake. More microbial omics studies are needed to  
564 compare the prediction power across different body sites and to understand how microbiome  
565 interact with metabolites differently at different body sites.  
566  
567 We are aware the data-preprocessing step has larger effects on the prediction performance. The  
568 distribution assumption, normalization, transformation, outlier filtering, and how to handle  
569 missing data are important to be considered before performing prediction. We have touched base  
570 on that, but potential further exploration may be needed.  
571  
572 The numbers of the measured metabolites and the numbers of the to-be predicted metabolites in  
573 each of the three studies are very different due to the difference of the technology platforms, and  
574 the available data. As what we proposed is not for causality but for mathematic prediction, we  
575 show examples of four metabolites (**Figure 8**) that may provide nutrition to species.  
576  
577 As a limitation, same as MelonnPan, the experimental design hasn't been considered in this  
578 framework for ENVIM, including time course or disease statuses. As the purpose of this study is  
579 prediction, it's reasonable to think that prediction is not necessary to be conditional on the  
580 experimental design. Instead, different disease statuses may have different microbiome profiles

581 and have corresponding different metabolomes. Therefore, this is a limitation but not a drawback  
582 of prediction performance. Another future direction is more of the metabolite set tests (or  
583 pathways analysis) according to the predicted metabolites.

584  
585 As a summary, we anticipate the newly developed ENVIM method for microbiome-based  
586 metabolite prediction provides good prediction performance and will be used to infer individual  
587 metabolites experimental design when only microbiome data are available, or in the condition  
588 that a proportion of samples in a study have no metabolome profile.

589  
590

### 591 **Acknowledgments**

592 We acknowledge NIH/NIDCR R03-DE02898, NIH/NIDCR U01-DE025046 and P30 CA016059  
593 (Massey Cancer Center Support Grant) for funding support. We also acknowledge that Prof  
594 William Valdar for supporting Jialiu Xie.

595

### 596 **Declaration of interests**

597 The authors declare no competing interests.

598

### 599 **Contribution to the Field Statement**

600 Microbiome data are becoming increasingly available in large health cohorts yet metabolomics  
601 data are still scant. While many studies generate microbiome data, they lack matched  
602 metabolomics data or have considerable missing proportions of metabolites. Since metabolomics  
603 is key to understanding microbial and general biological activities, the possibility of imputing  
604 individual metabolites from microbial taxonomy or metagenomics is intriguing. Importantly,  
605 current metabolomics profiling methods have unknown accuracy and are limited in their ability  
606 to predict individual metabolites. To address this gap, we developed a novel metabolite  
607 prediction method (ENVIM) based on the Elastic Net Model (ENM) using metagenomics,  
608 metatranscriptomics, or both data types. ENVIM introduces an extra step to ENM to consider  
609 variable importance scores and thus achieve better prediction power. The better prediction  
610 capability of ENVIM than the existing MelonPan in three datasets generated from oral, gut, and  
611 vaginal samples, suggest the potential usage in a variety of studies from different body sites. As a  
612 summary, we anticipate ENVIM provides good prediction performance, and will be used to infer  
613 individual metabolites experimental design when only microbiome data are available, or in the  
614 condition that a proportion of samples in a study have no metabolome data profile.

615  
616

### 617 **Figure and Table legend for main content**

618

619 **Figure 1.** Flowchart of data preprocessing in microbiome and metabolome  
620 Mallick didn't use QRILC, the other two used.

621

622 **Figure 2.** Flowchart of Melonpan and ENVIM. The three differences between them include  
623 (red text) (1) Transformation of metabolite data (2) Gene family weights and (3) Penalty score.  
624 The predictable metabolites are defined as the metabolites that have a significant Spearman  
625 correlation with the adjusted q-value (testing whether the correlation is zero) below the default  
626 threshold in the training set.

627

628 **Figure 3.** (a) Boxplot of -log10 of shapiro test p-values for relative metabolites abundances in all  
629 three data applied with box-cox transformation (we used) and arcsin square root transformation  
630 (Melonnpn used). (b) Scatter plot for comparing -log10 of p-values made by shapiro test  
631 (normality) between box-cox transformation (x-axis) and arcsin sqrt (y-axis) transformation.  
632 Almost all of the points are above the  $y = x$  line, which means that the -log10 of p-value after  
633 box-cox transformation is smaller than after arcsin sqrt transformation, and normality after box-  
634 cox transformation is better.

635

636 **Figure 4.** Evaluation using Spearman correlation in training stage and testing stage between  
637 predicted values and the observed values by using DNaseq data only, RNAseq data only, and  
638 both for ZOE2.0 data, Lloyd-Price Data, and Mallick data.

639

640 **Figure 5.** For DNA, RNA, and both in each study and the training set, this shows the scatter plot  
641 of Spearman correlation in ENVIM (y-axis) and Melonnpn (x-axis). Spearman correlation is  
642 based on observed metabolite abundance and predicted values. If our calculated correlation is  
643 NA, the metabolites will be included in this figure.

644

645 **Figure 6.** For DNA, RNA, and both in each study and the testing set, this shows the scatter plot  
646 of Spearman correlation in ENVIM (y-axis) and Melonnpn (x-axis). Spearman correlation is  
647 based on observed metabolite abundance and predicted values.

648

649 **Figure 7.** The best predicted 50 metabolite compounds (x-axis) in the three studies by ENVIM in  
650 the testing set. For Lloyd-Price and ZOE2.0, we choose the gene family data types that have the  
651 best ENVIM prediction power to show their top predicted metabolites, based on **Table 2**.

652

653 **Figure 8.** Scatter plots of examples of well-predicted metabolites in ZOE 2.0 by ENVIM. The X-  
654 axis is observed metabolites; the y-axis is for predicted metabolites. Both are in log10 scale of  
655 the compositional data for normality. ECC is for Early Childhood Caries, ECC =0 (about 50% of  
656 total samples in ZOE 2.0) is for the healthy group, and ECC=1 (about 50% of total samples in  
657 ZOE 2.0) is for the ECC case group. r is for Spearman correlation.

658

659 **Figure 9.** Taxonomic enrichment of metabolite predictive species for the most contributing  
660 species to metabolite prediction, based on ZOE2.0 DNA or RNA by ENVIM. The top 20  
661 significant over-represented bacteria with the smallest Q values ( $Q < 0.05$ ) for ZOE 2.0 data. The  
662 Q-value is based on the Kolmogorov-Smirnov (KS) test p values after FDR correction. (a) DNA  
663 data (b) RNA data.

664

665 **Table 1. Sample size and number of selected gene family features.**

666 Testing genes: genes can be used in the testing set.

667 Training genes: genes can be used in the training set.

668 Genes in both: genes are in both training and testing sets.

669

670 **Table 2.** Prediction results (first four columns of numbers) in terms of Spearman correlation for  
671 all metabolites to be predicated. Based on the “well-prediction” criterion, defined as Spearman  
672 correlation  $> 0.3$  between the observed and the predicted metabolites, the numbers of well-

673 predicted metabolites with different prediction methods, datasets, and modality levels (DNA,  
674 RNA, and BOTH), are presented for comparing MelonnPan and ENVIM. NM is the number of  
675 metabolites to be predicted. Percentages in parentheses (%) represent the number of well-  
676 predicted metabolites divided by the total number of metabolites (NM) to be predicted in each  
677 study. The Mallick cohort has only metagenomics data available.  
678 The last column of numbers is for the numbers of "predicable metabolites", that are defined by  
679 MelonnPan, also seen in the **Figure 2** legend.  
680

681 **Table 3.** Prediction results via Spearman correlation for metabolites that are found in metabolic  
682 pathways. Based on the criterion of Spearman correlation  $>0.3$  between observed and predicted  
683 metabolites, we present the numbers of well-predicted metabolites with different prediction  
684 methods, datasets, and modality levels (DNA, RNA, and both), and comparing between  
685 MelonnPan and ENVIM. NM is the number of metabolites to be predicted. Percentages in  
686 parentheses (%) represent the numbers of well-predicted metabolites divided by the total number  
687 of metabolites (NM) to be predicted in each study. The Mallick cohort has only metagenomics  
688 (DNA) data available and no pathway RNA data. The results from the Mallick cohort here are  
689 only based on filters (filtering out metabolites with mean relative abundance  $<10^{-4}$ ) and low  
690 prevalence (metabolites with  $>10\%$  non-zero). In ZOE 2.0 and Lloyd-Price, metabolite data  
691 presented in this table have been selected according to membership in pathways and also satisfy  
692 the above-mentioned filtering criteria.  
693  
694

### 695 **Figure and Table legend for supplemental files**

696  
697 **Supplemental Figure 1.** Boxplot of  $-\log_{10}$  of mean square error for DNA, RNA, and Both in  
698 each of the three studies. None of the nominal p values to compare ENVIM and MelonnPan are  
699 significant as all of them  $>0.1$ .  
700

701 **Supplemental Figure 2.** Diagnosis for outlier samples. The X-axis is the cumulative proportion  
702 of samples, and the y-axis is number of non-missing values. The left lower tail dots that are far  
703 from the rest may be considered as sample outliers. For ZOE 2.0 data and Lloyd-Price data, we  
704 need to remove the 10 outliers subjects from ZOE 2.0 data and 15 outliers from Lloyd-Price data  
705 to ensure the distribution of non-missing values is continuous.  
706

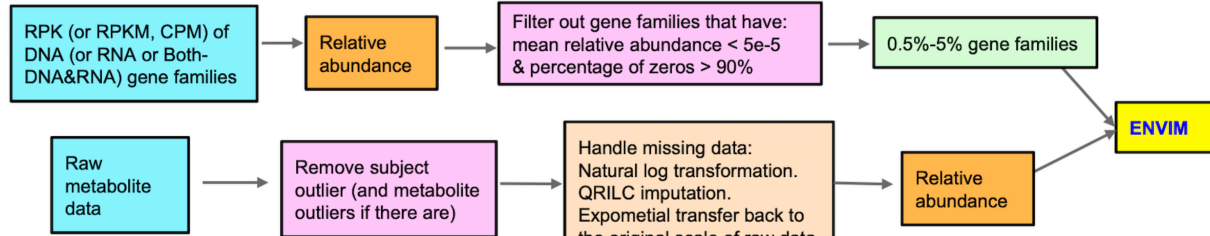
707 **Supplemental Table 1.** Overall prediction results, for all gene family data types, all three  
708 datasets, and both methods, in Spearman correlation and MSE.  
709

710 **Supplemental Table 2.** The gene lists in DNA or RNA, based on the highest rank or the average  
711 rank among metabolites, that contribute to metabolite prediction in ZOE 2.0 by ENVIM. Rank is  
712 based on the weight matrix in ENVIM. A larger number of ranks suggests more important gene  
713 families.  
714  
715  
716  
717  
718

719

Figure 1

Data Pre-processing



720

721

722

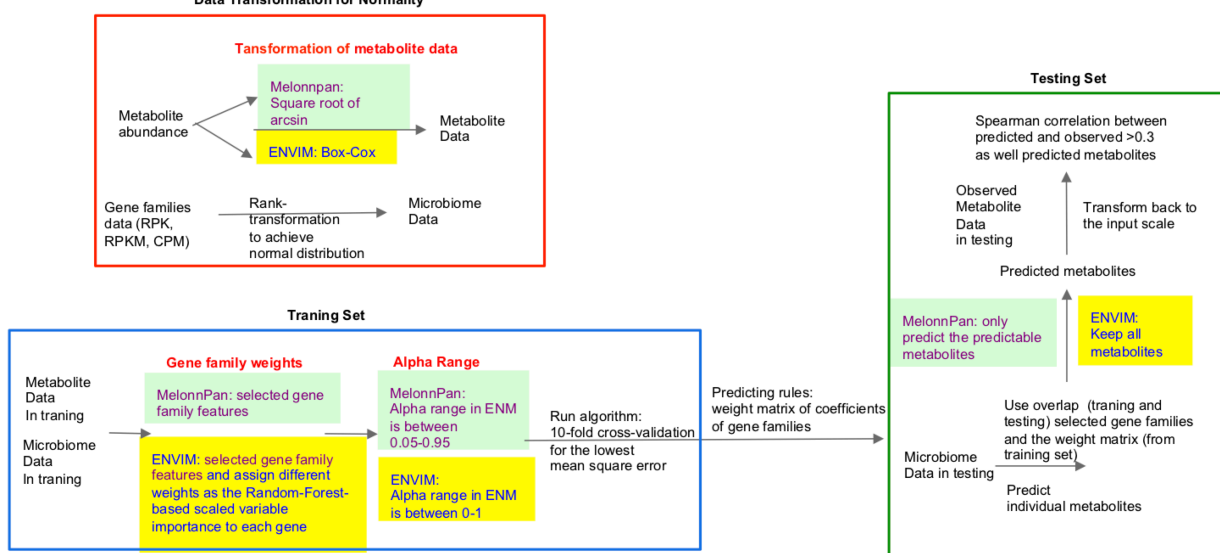
723

724

725

Figure 2

Data Transformation for Normality



726

727

728

729

730

731

732

733

734

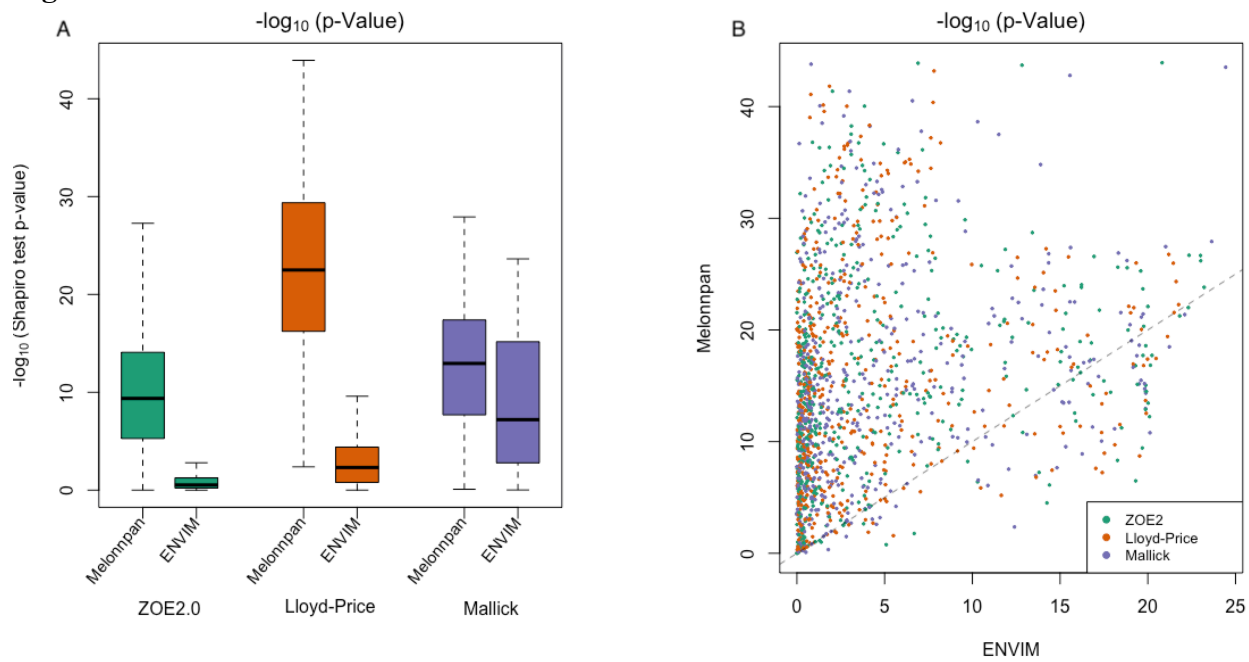
735

736

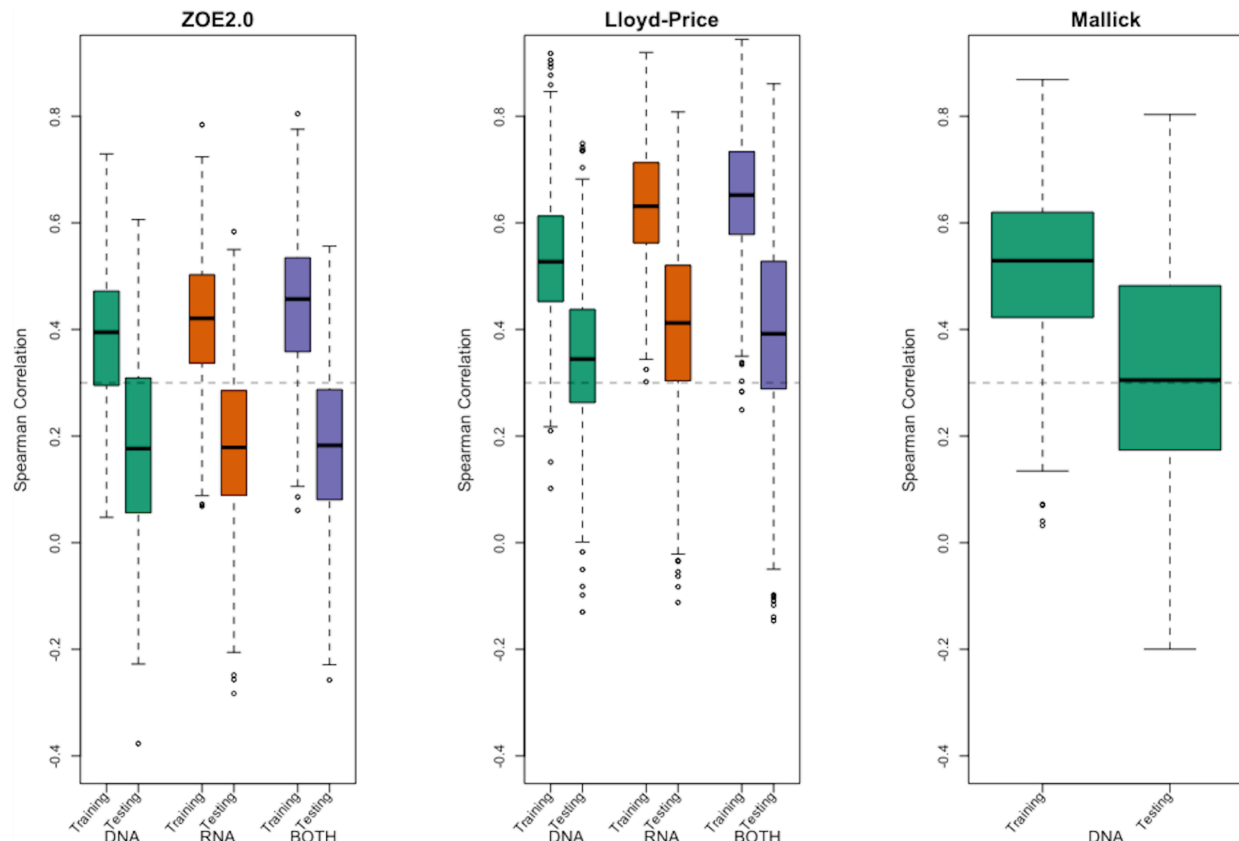
737

738

739 **Figure 3**

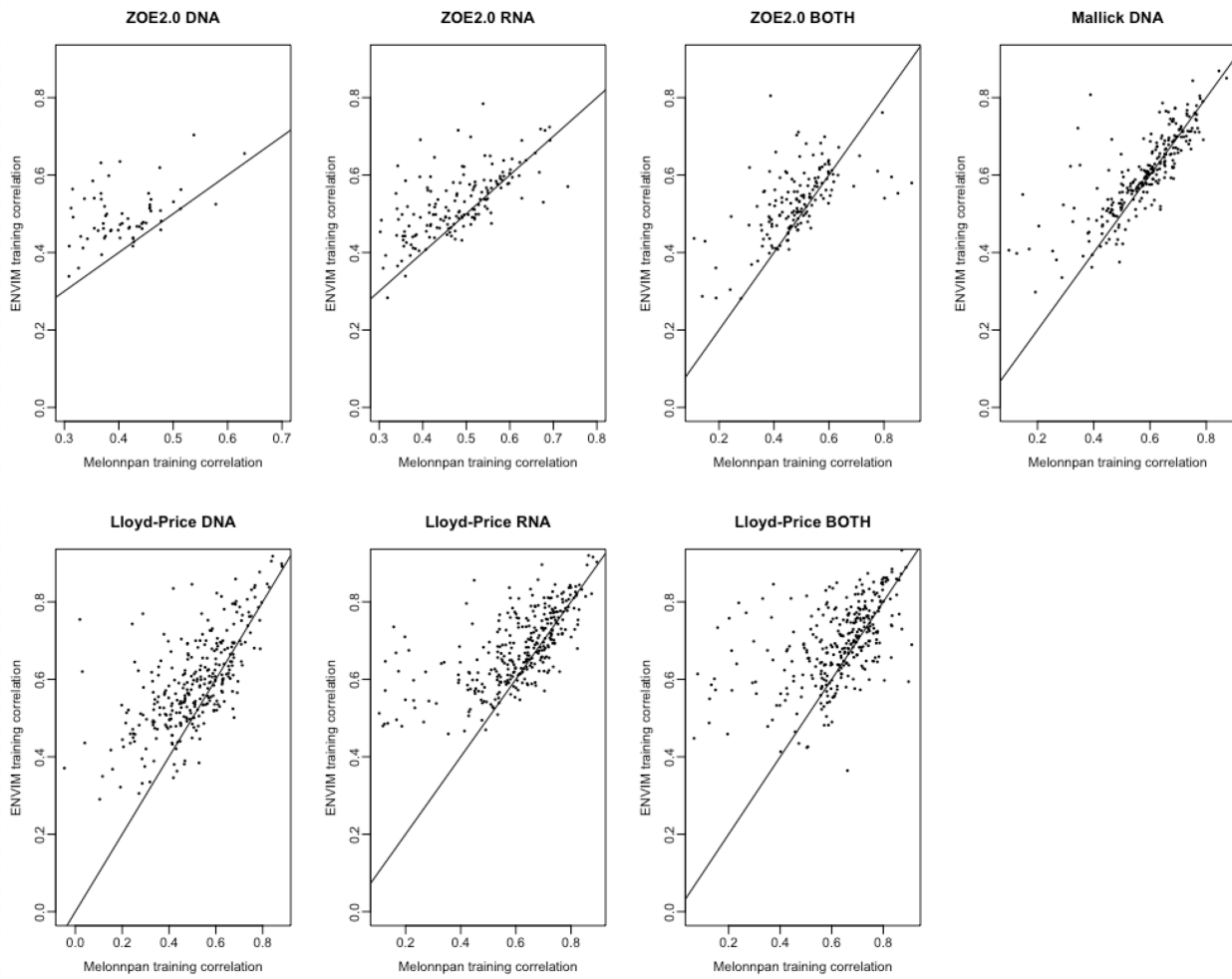


740  
741  
742  
743  
744 **Figure 4**  
745



746

747 **Figure 5**



748

749

750

751

752

753

754

755

756

757

758

759

760

761

762

763

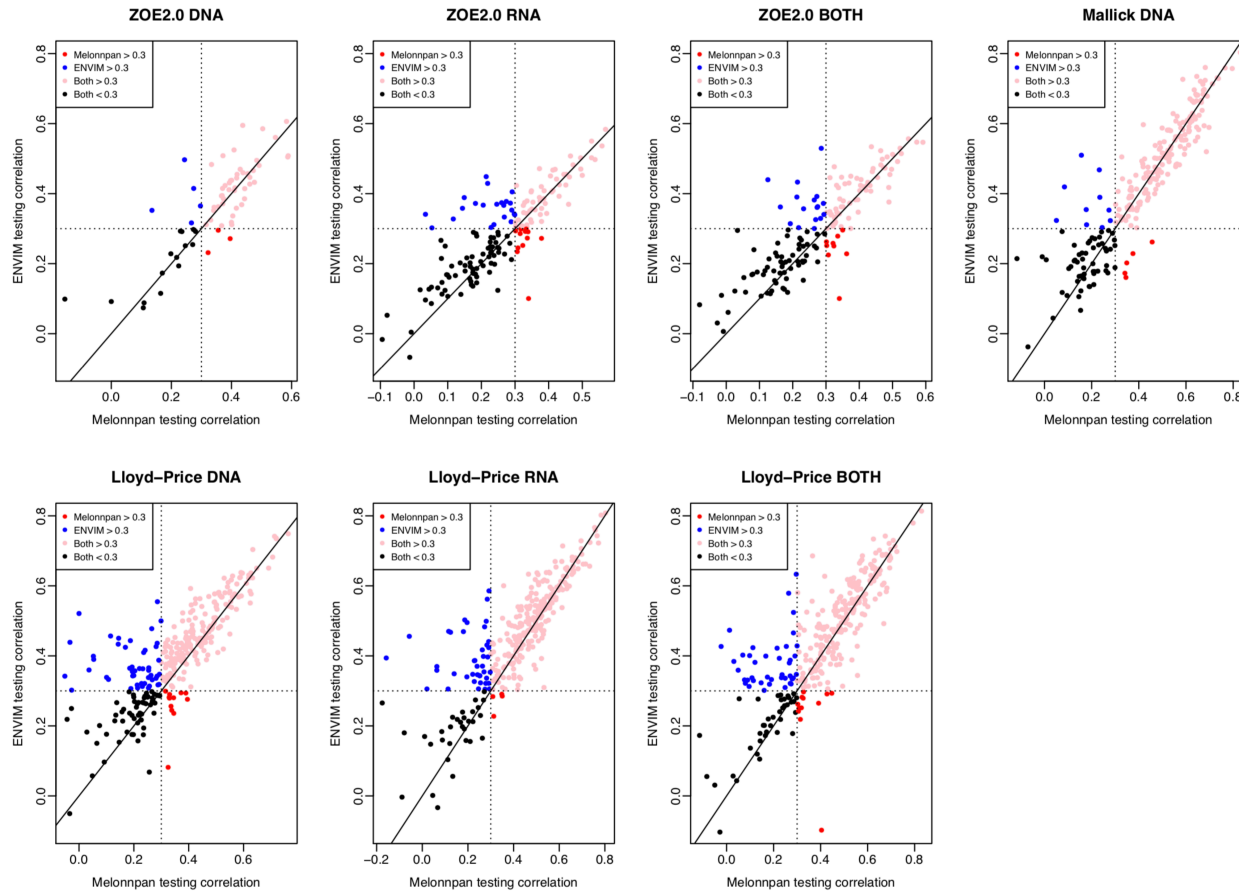
764

765

766

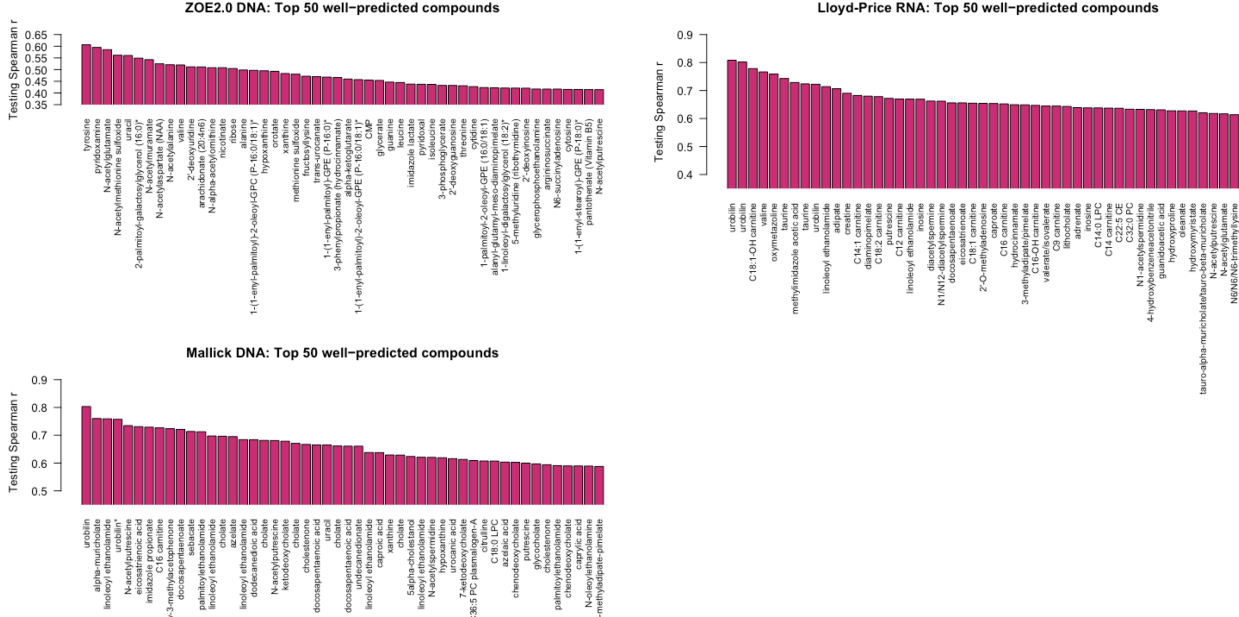
767

768 **Figure 6**



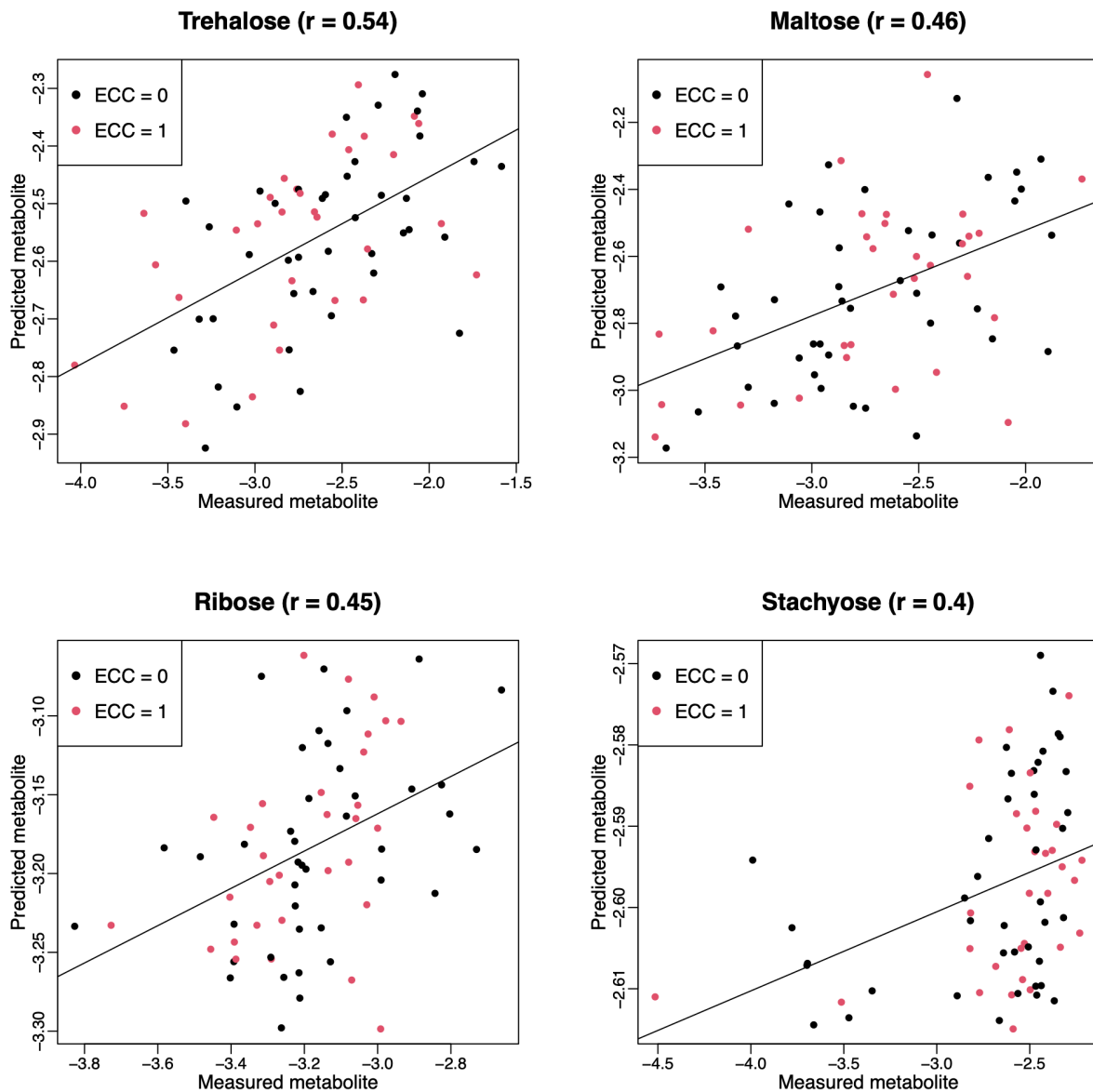
769  
770  
771  
772

**Figure 7**



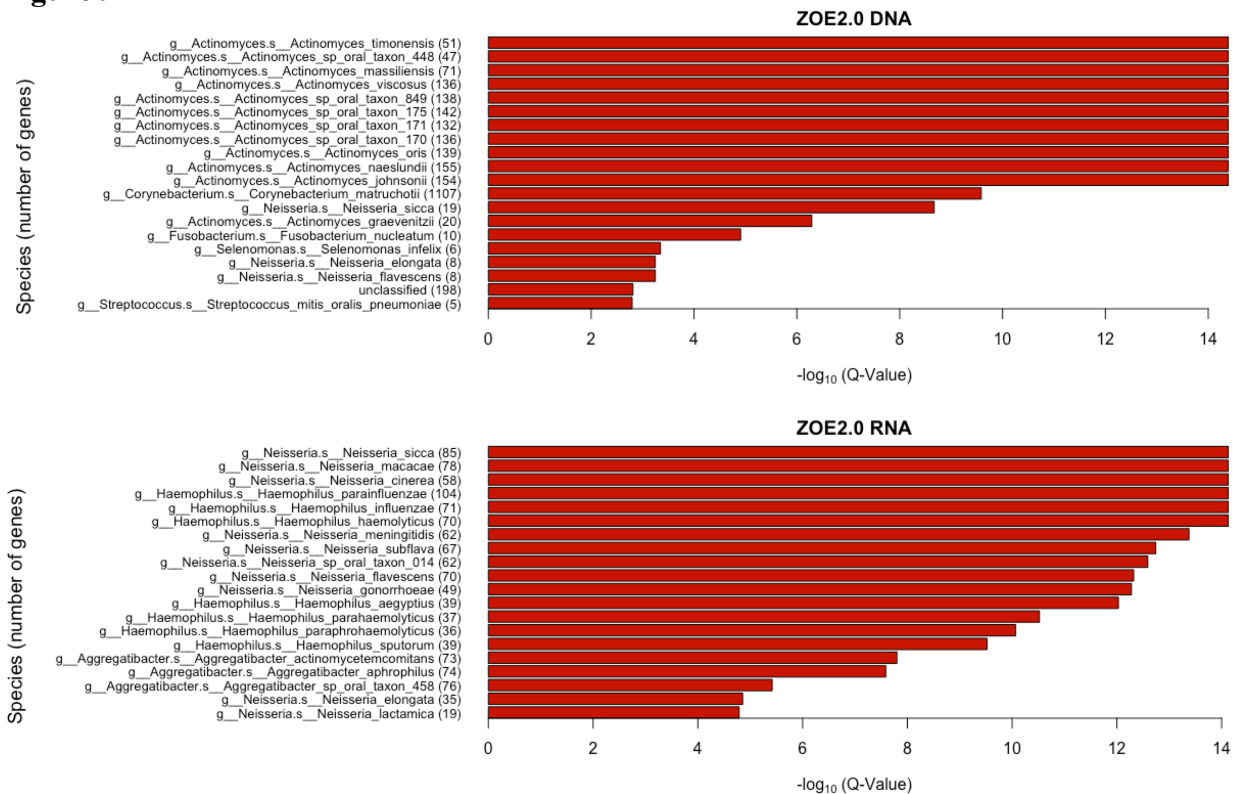
773

774 **Figure 8**



775  
776  
777  
778  
779  
780  
781  
782  
783  
784  
785  
786  
787

788 **Figure 9**



789  
790  
791  
792  
793  
794  
795  
796  
797  
798  
799  
800  
801  
802  
803  
804  
805  
806  
807  
808  
809  
810  
811  
812

		Training genes	Testing genes	Genes in both	Subjects	Metabolites	Metabolites (in pathways)
ZOE 2.0	DNA (total 403k genes)	1355	1276	1214	289	503	149
	RNA (total 403k genes)	1805	1826	1667	287	503	149
	BOTH (total 806k genes)	3158	3183	2948	287	503	149
Lloyd-Price	DNA (total 2741k genes)	726	712	633	359	522	125
	RNA (total 1079k genes)	726	704	600	282	522	125
	BOTH (total 3820k genes)	1424	1508	1211	269	522	125
Mallick	DNA (total 1000k genes)	811	811	811	220	466	251 (Filter Only)

813 **Table 1**

814

815

816

817

818

819

820

821

822

823

824

825

826

827

828

829

830

831

832

ZOE 2.0 (NM=503)	Training (ENVIM)	Training (MelonnPan)	Testing (ENVIM)	Testing (MelonnPan)	Predictable metabolites (Defined by MelonnPan)
DNA only	356 (71%)	63 (13%)	<b>124 (25%)</b>	47 (9%)	70
RNA only	409 (81%)	157 (31%)	106 (21%)	68 (14%)	163
BOTH DNA and RNA	423 (84%)	146 (29%)	110 (22%)	73 (15%)	154
Mallick Cohort (NM=466)					
DNA only	408 (88%)	239 (51%)	225 (48%)	178 (38%)	249
Lloyd-Price Cohort (NM=522)					
DNA only	501 (96%)	271 (52%)	322 (62%)	193 (37%)	305
RNA only	521 (100%)	298 (57%)	<b>393 (75%)</b>	236 (45%)	318
BOTH DNA and RNA	518 (99%)	306 (59%)	381 (73%)	232 (44%)	323

833

**Table 2**

834

835

836

837

838

839

840

841

ZOE 2.0 (NM=149)	Training (ENVIM)	Training (MelonnPan)	Testing (ENVIM)	Testing (MelonnPan)
DNA only	128 (86%)	44 (30%)	46 (31%)	24 (16%)
RNA only	140 (94%)	83 (56%)	59 (40%)	43 (29%)
Both DNA and RNA	143 (96%)	81 (54%)	64 (43%)	45 (30%)
Mallick Cohort (NM=251)				
DNA only	231 (92%)	132 (53%)	94 (37%)	71 (28%)
Lloyd-Price Cohort (NM=125)				
DNA only	123 (98%)	102 (82%)	75 (60%)	74 (59%)
RNA only	125 (100%)	110 (88%)	102 (82%)	93 (74%)
Both DNA and RNA	125 (100%)	110 (88%)	107 (86%)	96 (77%)

842

**Table 3**

843

844

845 **References**

846

847 1. Wilkinson JE, Franzosa EA, Everett C, Li C, Hu FB, Wirth DF, et al. A framework for  
848 microbiome science in public health. *Nature Medicine*. 2021;27(5):766-74.

849 2. Lloyd-Price J, Arze C, Ananthakrishnan AN, Schirmer M, Avila-Pacheco J, Poon TW, et  
850 al. Multi-omics of the gut microbial ecosystem in inflammatory bowel diseases. *Nature*.  
851 2019;569(7758):655-62.

852 3. Canfora EE, Meex RCR, Venema K, Blaak EE. Gut microbial metabolites in obesity,  
853 NAFLD and T2DM. *Nat Rev Endocrinol*. 2019;15(5):261-73.

854 4. Kenny DJ, Plichta DR, Shungin D, Koppel N, Hall AB, Fu B, et al. Cholesterol  
855 Metabolism by Uncultured Human Gut Bacteria Influences Host Cholesterol Level. *Cell Host  
856 Microbe*. 2020;28(2):245-57.e6.

857 5. Heimisdottir LH, Lin BM, Cho H, Orlenko A, Ribeiro AA, Simon-Soro A, et al.  
858 Metabolomics Insights in Early Childhood Caries. *J Dent Res*. 2021;100(6):615-22.

859 6. Franzosa EA, McIver LJ, Rahnavard G, Thompson LR, Schirmer M, Weingart G, et al.  
860 Species-level functional profiling of metagenomes and metatranscriptomes. *Nature methods*.  
861 2018;15(11):962-8.

862 7. Thomas AM, Manghi P, Asnicar F, Pasolli E, Armanini F, Zolfo M, et al. Metagenomic  
863 analysis of colorectal cancer datasets identifies cross-cohort microbial diagnostic signatures and  
864 a link with choline degradation. *Nature Medicine*. 2019;25(4):667-78.

865 8. Noecker C, Eng A, Srinivasan S, Theriot CM, Young VB, Jansson JK, et al. Metabolic  
866 model-based integration of microbiome taxonomic and metabolomic profiles elucidates  
867 mechanistic links between ecological and metabolic variation. *MSystems*. 2016;1(1):e00013-15.

868 9. Mallick H, Franzosa EA, McIver LJ, Banerjee S, Sirota-Madi A, Kostic AD, et al.  
869 Predictive metabolomic profiling of microbial communities using amplicon or metagenomic  
870 sequences. *Nat Commun*. 2019;10(1):3136.

871 10. Sanna S, van Zuydam NR, Mahajan A, Kurilshikov A, Vila AV, Võsa U, et al. Causal  
872 relationships among the gut microbiome, short-chain fatty acids and metabolic diseases. *Nature  
873 genetics*. 2019;51(4):600-5.

874 11. Divaris K, Slade GD, Ferreira Zandona AG, Preisser JS, Ginnis J, Simancas-Pallares  
875 MA, et al. Cohort Profile: ZOE 2.0-A Community-Based Genetic Epidemiologic Study of Early  
876 Childhood Oral Health. *Int J Environ Res Public Health*. 2020;17(21).

877 12. Divaris K, Joshi A. The building blocks of precision oral health in early childhood: the  
878 ZOE 2.0 study. *J Public Health Dent*. 2020;80 Suppl 1:S31-s6.

879 13. Ginnis J, Ferreira Zandoná AG, Slade GD, Cantrell J, Antonio ME, Pahel BT, et al.  
880 Measurement of Early Childhood Oral Health for Research Purposes: Dental Caries Experience  
881 and Developmental Defects of the Enamel in the Primary Dentition. *Methods Mol Biol*.  
882 2019;1922:511-23.

883 14. Divaris K, Shungin D, Rodríguez-Cortés A, Basta PV, Roach J, Cho H, et al. The  
884 Supragingival Biofilm in Early Childhood Caries: Clinical and Laboratory Protocols and  
885 Bioinformatics Pipelines Supporting Metagenomics, Metatranscriptomics, and Metabolomics  
886 Studies of the Oral Microbiome. *Methods Mol Biol*. 2019;1922:525-48.

887 15. Evans AM, Bridgewater B, Liu Q, Mitchell M, Robinson R, Dai H, et al. High resolution  
888 mass spectrometry improves data quantity and quality as compared to unit mass resolution mass  
889 spectrometry in high-throughput profiling metabolomics. *Metabolomics*. 2014;4(2):1.

890 16. Evans AM, DeHaven CD, Barrett T, Mitchell M, Milgram E. Integrated, nontargeted  
891 ultrahigh performance liquid chromatography/electrospray ionization tandem mass spectrometry  
892 platform for the identification and relative quantification of the small-molecule complement of  
893 biological systems. *Analytical chemistry*. 2009;81(16):6656-67.

894 17. Franzosa EA, Sirota-Madi A, Avila-Pacheco J, Fornelos N, Haiser HJ, Reinker S, et al.  
895 Gut microbiome structure and metabolic activity in inflammatory bowel disease. *Nature  
896 Microbiology*. 2019;4(2):293-305.

897 18. Wei R, Wang J, Su M, Jia E, Chen S, Chen T, et al. Missing Value Imputation Approach  
898 for Mass Spectrometry-based Metabolomics Data. *Sci Rep*. 2018;8(1):663.

899 19. Zou H, Hastie T. Regularization and variable selection via the elastic net. *Journal of the  
900 royal statistical society: series B (statistical methodology)*. 2005;67(2):301-20.

901 20. Cohen J. *Statistical Power Analysis for the Behavioral Sciences*. Hillsdile. Erlbaum.  
902 Conner, BE (1988). *The Box in the Barn*. Columbus: Highlights for ...; 1988.

903 21. Aulchenko YS, Ripke S, Isaacs A, Van Duijn CM. GenABEL: an R library for genome-  
904 wide association analysis. *Bioinformatics*. 2007;23(10):1294-6.

905 22. Breiman L. Random forests. *Machine learning*. 2001;45(1):5-32.

906 23. Kuhn M. Building predictive models in R using the caret package. *J Stat Softw*.  
907 2008;28(5):1-26.

908 24. Friedman J, Hastie T, Tibshirani R. Regularization paths for generalized linear models  
909 via coordinate descent. *Journal of statistical software*. 2010;33(1):1.

910